

NOAA Technical Memorandum ERL GLERL-34

IMPROVED ST. CLAIR RIVER DYNAMICS FLOW MODELS
AND COMPARISON ANALYSIS

J. A. Derecki
R. N. Kelley

Great Lakes Environmental Research Laboratory
Ann Arbor, Michigan
May 1981



UNITED STATES
DEPARTMENT OF COMMERCE
Malcolm Baldrige,
Secretary

NATIONAL OCEANIC AND
ATMOSPHERIC ADMINISTRATION
James P. Walsh,
Acting Administrator

Environmental Research
Laboratories
Joseph O. Fletcher,
Acting Director

NOTICE

The NOAA Environmental Research Laboratories do not approve, recommend, or endorse any proprietary product or proprietary material mentioned in this publication. No reference shall be made to the NOAA Environmental Research Laboratories, or to this publication furnished by the NOAA Environmental Research Laboratories, in any advertising or sales promotion which would indicate or imply that the NOAA Environmental Research Laboratories approve, recommend, or endorse any proprietary product or proprietary material mentioned herein, or which has as its purpose an intent to cause directly or indirectly the advertised product to be used or purchased because of this NOAA Environmental Research Laboratories publication.

TABLE OF CONTENTS

	Page
Abstract	1
1. INTRODUCTION	2
2. PROCEDURE	2
3. RESULTS	5
3.1 Model Calibration	5
3.2 Computer Programs	6
3.3 Comparison of NEW and OLD Models	9
3.4 Wind Stress Effects	11
3.5 Time Scale Effects	12
3.6 Effect of Daiiy Winds on Hourly Models	13
3.7 Comparison of Different Models	14
4. CONCLUSIONS	21
5. REFERENCES	23
Appendix A. GENERALIZED ST. CLAIR RIVER DAILY FLOW MODEL, INPUT, AND OUTPUT	24

FIGURES

(Prefixes M and A indicate microfiche and appendix figures, respectively.)

		Page
1.	Manning's roughness coefficient for the Fort Gratiot-Mouth of Black River reach.	7
2.	Manning's roughness coefficient for the Dunn Paper-Mouth of Black River reach.	7
3.	Manning's roughness coefficient for the Mouth of Black River-Dry Dock reach.	8
4.	Manning's roughness coefficient for the Dry Dock-St. Clair reach.	8
M-5a.	Histogram of NEW and OLD model differences on daily flow computations: Model 1, daily time scale, NEW - OLD.	Inside Back Cover
M-5b.	Cumulative frequency curve for NEW and OLD model differences on daily flow computations: Model 1, daily time scale.	Inside Back Cover
M-6a.	Histogram of NEW and OLD model differences on daily flow computations: Model 1, hourly time scale, NEW - OLD.	Inside Back Cover
M-6b.	Cumulative frequency curve for NEW and OLD model differences on daily flow computations: Model 1, hourly time scale.	Inside Back Cover
M-7a.	Histogram of NEW and OLD model differences on daily flow computations: Model 3, daily time scale, NEW - OLD.	Inside Back Cover
M-7b.	Cumulative frequency curve for NEW and OLD model differences on daily flow computations: Model 3, daily time scale.	Inside Back Cover
M-8a.	Histogram of NEW and OLD model differences on daily flow computations: Model 3, hourly time scale, NEW - OLD.	Inside Back Cover
M-8b.	Cumulative frequency curve for NEW and OLD model differences on daily flow computations: Model 3, hourly time scale.	Inside Back Cover
M-9a.	Histogram of wind effects on daily flow computations: Model 1, daily time scale, wind - no wind.	Inside Back Cover
M-9b.	Cumulative frequency curve for wind effects on daily flow computations: Model 1, daily time scale.	Inside Back Cover

FIGURES--Continued

	Page
M-10a. Histogram of wind effects on daily flow computations: Model 1, hourly time scale, wind - no wind.	Inside Back Cover
M-10b. Cumulative frequency curve for wind effects on daily flow computations: Model 1, hourly time scale.	Inside Back Cover
M-11a. Histogram of wind effects on daily flow computations: Model 2, daily time scale, wind - no wind.	Inside Back Cover
M-11b. Cumulative frequency curve for wind effects on daily flow computations: Model 2, daily time scale.	Inside Back Cover
M-12a. Histogram of wind effects on daily flow computations: Model 2, hourly time scale, wind - no wind.	Inside Back Cover
M-12b. Cumulative frequency curve for wind effects on daily flow computations: Model 2, hourly time scale.	Inside Back Cover
M-13a. Histogram of wind effects on daily flow computations: Model 3, daily time scale, wind - no wind.	Inside Back Cover
M-13b. Cumulative frequency curve for wind effects on daily flow computations: Model 3, daily time scale.	Inside Back Cover
M-14a. Histogram of wind effects on daily flow computations: Model 3, hourly time scale, wind - no wind.	Inside Back Cover
M-14b. Cumulative frequency curve for wind effects on daily flow computations: Model 3, hourly time scale.	Inside Back Cover
M-15.a. Histogram of daily and hourly time scale effects on daily flow computations : Model 1, no wind, daily - hourly.	Inside Back Cover
M-15b. Cumulative frequency curve for daily and hourly time scale effects on daily flow computations: Model 1, no wind.	Inside Back Cover
M-16a. Histogram of daily and hourly time scale effects of daily flow computations: Model 1, wind, daily - hourly.	Inside Back Cover
M-16b. Cumulative frequency curve for daily and hourly time scale effects on daily flow computations: Model 1, wind.	Inside Back Cover
M-17a. Histogram of daily and hourly time scale effects on daily flow computations: Model 2, no wind, daily - hourly.	Inside Back Cover

FIGURES--Continued

	Page
M-17b. Cumulative frequency curve for daily and hourly time scale effects on daily flow computations: Model 2, no wind.	Inside Back Cover
M-18a. Histogram of daily and hourly time scale effects on daily flow computations: Model 2, wind, daily - hourly.	Inside Back Cover
M-18b. Cumulative frequency curve for daily and hourly time scale effects on daily flow computations: Model 2, wind.	Inside Back Cover
M-19a. Histogram of daily and hourly time scale effects on daily flow computations: Model 3, no wind, daily - hourly.	Inside Back Cover
M-19b. Cumulative frequency curve for daily and hourly time scale effects on daily flow computations: Model 3, no wind.	Inside Back Cover
M-20a. Histogram of daily and hourly time scale effects on daily flow computations: Model 3, wind, daily - hourly.	Inside Back Cover
M-20b. Cumulative frequency curve for daily and hourly time scale effects on daily flow computations: Model 3, wind.	Inside Back Cover
M-21a. Histogram of daily and hourly time scale effects on daily flow computations: Model OLD 1, no wind, daily - hourly.	Inside Back Cover
M-21b. Cumulative frequency curve for daily and hourly time scale effects on daily flow computations: Model OLD 1, no wind.	Inside Back Cover
M-22a. Histogram of daily and hourly time scale effects on daily flow computations: Model OLD 3, no wind, daily - hourly.	Inside Back Cover
M-22b. Cumulative frequency curve for daily and hourly time scale effects on daily flow computations: Model OLD 3, no wind.	Inside Back Cover
M-23a. Histogram of effects for daily wind in hourly time scale models on daily flow computations: Model 1, daily - hourly wind.	Inside Back Cover

FIGURES--Continued

	Page
M-23b. Cumulative frequency curve for effects of daily wind in hourly time scale models on daily flow computations: Model 1.	Inside Back Cover
M-24a. Histogram of effects for daily wind in hourly time scale models on daily flow computations: Model 2, daily - hourly wind.	Inside Back Cover
M-24b. Cumulative frequency curve for effects of daily wind in hourly time scale models on daily flow computations: Model 2.	Inside Back Cover
M-25a. Histogram of effects for daily wind in hourly time scale models on daily flow computations: Model 3, daily - hourly wind.	Inside Back Cover
M-25b. Cumulative frequency curve for effects of daily wind in hourly time scale models on daily flow computations: Model 3.	Inside Back Cover
M-26a. Histogram of different model and configuration effects on daily flow computations: Model 1 - 2, daily, no wind.	Inside Back Cover
M-26b. Cumulative frequency curve for different model and configuration effects on daily flow computations: Model 1 - 2, daily, no wind.	Inside Back Cover
M-27a. Histogram of different model and configuration effects on daily flow computations: Model 1 - 2, daily, wind.	Inside Back Cover
M-27b. Cumulative frequency curve for different model and configuration effects on daily flow computations: Model 1 - 2, daily, wind.	Inside Back Cover
M-28a. Histogram of different model and configuration effects on daily flow computations: Model 1 - 2, hourly, no wind.	Inside Back Cover
M-28b. Cumulative frequency curve for different model and configuration effects on daily flow computations: Model 1 - 2, hourly, no wind.	Inside Back Cover
M-29a. Histogram of different model and configuration effects on daily flow computations: Model 1 - 2, hourly, wind.	Inside Back Cover
M-29b. Cumulative frequency curve for different model and configuration effects on daily flow computations: Model 1 - 2, hourly, wind.	Inside Back Cover

FIGURES--Continued

	Page
M-30a. Histogram of different model and configuration effects on daily flow computations: Model 1 - 3, daily, no wind	Inside Back Cover
M-30b. Cumulative frequency curve for different model and configuration effects on daily flow computations: Model 1 - 3, daily, no wind.	Inside Back Cover
M-31.9. Histogram of different model and configuration effects on daily flow computations: Model 1 - 3, daily, wind.	Inside Back Cover
M-31b. Cumulative frequency curve for different model and configuration effects on daily flow computations: Model 1 - 3, daily, wind.	Inside Back Cover
M-32a. Histogram of different model and configuration effects on daily flow computations: Model 1 - 3, hourly, no wind.	Inside Back Cover
M-32b. Cumulative frequency curve for different model and configuration effects on daily flow computations: Model 1 - 3, hourly, no wind.	Inside Back Cover
M-33a. Histogram of different model and configuration effects on daily flow computations: Model 1 - 3, hourly, wind.	Inside Back Cover
M-33b. Cumulative frequency curve for different model and configuration effects on daily flow computations: Model 1 - 3, hourly, wind.	Inside Back Cover
M-34a. Histogram of different model and configuration effects on daily flow computations: Model 2 - 3, daily, no wind.	Inside Back Cover
M-34b. Cumulative frequency curve for different model and configuration effects on daily flow computations: Model 2 - 3, daily, no wind.	Inside Back Cover
M-35a. Histogram of different model and configuration effects on daily flow computations: Model 2 - 3, daily, wind.	Inside Back Cover
M-35b. Cumulative frequency curve for different model and configuration effects on daily flow computations: Model 2 - 3, daily, wind.	Inside Back Cover
M-36a. Histogram of different model and configuration effects on daily flow computations: Model 2 - 3, hourly, no wind.	Inside Back Cover

FIGURES--Continued

	Page
M-36b. Cumulative frequency curve for different model and configuration effects on daily flow computations: Model 2 - 3, hourly, no wind.	Inside Back Cover
M-37a. Histogram of different model and configuration effects on daily flow computations: Model 2 - 3, hourly, wind.	Inside Back Cover
M-37b. Cumulative frequency curve for different model and configuration effects on daily flow computations: Model 2 - 3, hourly, wind.	Inside Back Cover
M-38a. Histogram of different model and configuration effects on daily flow computations: Model OLD 1 - 3, daily, no wind.	Inside Back Cover
M-38b. Cumulative frequency curve for different model and configuration effects on daily flow computations: Model OLD 1 - 3, daily, no wind.	Inside Back Cover
M-39a. Histogram of different model and configuration effects on daily flow computations: Model OLD 1 - 3, hourly, no wind.	Inside Back Cover
M-39b. Cumulative frequency curve for different model and configuration effects on daily flow computations: Model OLD 1 - 3, hourly, no wind.	Inside Back Cover
40. Comparison of falls for upper and lower reaches of Model 1.	17
41. Comparison of falls for upper and lower reaches of Model 2.	18
42. Comparison of falls for upper and lower reaches of Model 3.	19
43. Comparison of water level differences between Lakeport and Fort Gratiot gages.	20
A-44. Generalized St. Clair River daily flow model.	26

TABLES

(Prefix A indicates appendix table.)

	Page
1. St. Clair River hydraulic parameters.	4
2. St. Clair River Manning's roughness coefficients.	9
3. Comparison of daily flows computed by NEW and OLD models: NEW - OLD.	10
4. Comparison of wind stress effects on daily flow computations: Wind - no wind.	12
5. Comparison of daily and hourly time scales on daily flow computations: Daily - hourly.	13
6. Comparison of daily flows computed with hourly models using daily and hourly winds: Daily - hourly.	14
J. Comparison of daily flows computed with different models and configurations.	15
8. Seasonal comparison of daily flows computed by NEW models with configuration: Daily, no wind.	22
A-Y. St. Clair River daily model output for Model 1 with wind stress, metric, December 1978.	25

IMPROVED ST. CLAIR RIVER DYNAMIC FLOW MODELS AND COMPARISON ANALYSIS*

Jan A. Derecki and Raymond N. Kelley

The St. Clair River dynamic flow models, modified to provide better channel definition, to include additional discharge measurements for model calibration, and to incorporate wind stress effects on river flows, are described and compared for daily flow differences resulting from channel definition improvements, wind effects, time scale effects, and a combination of these factors. All the St. Clair River models are derived for the upper river channel, spanning approximately one-third of the river. Model 1, with the steepest river slope, is for the headwaters (upper) reach; Model 2 overlaps most of the same reach, but starts farther down the river; finally, Model 3, with reduced slope, covers the lower reach. Model improvements due to additional measurements and better channel definition produced somewhat higher river flows, averaging 3 percent and 4 percent for the upper and lower models, respectively. The effects of wind stress and the selection of daily or hourly computational time scales are generally insignificant, with highest effects for the lower model, where wind produced a small increase (1 percent) in the number of days with significant flow differences. This difference is defined as a flow difference in excess of 2 percent of the total flow, which represents practical accuracy for flow measurements. The largest flow differences are obtained from comparisons of different models, with only a small influence exerted by various model configurations (wind, time scale). The number of days with significant flow differences for all comparisons between various models was 45 percent, varying between 54 percent, 48 percent, and 35 percent for Models 1 - 2, 1 - 3, and 2 - 3, respectively. These large percentages of days with significant flow differences are reduced drastically for higher percent flow differences (10-percent average at the 5-percent level) and are caused to a large extent by ice effects during winter. Generally, the accuracy of various models is compatible within 5 percent of flow for the open-water season, but may exceed 15 percent of flow for the ice-cover season because of ice effects. Model 1, with the upper gage nearly on the lake and the steepest river slope, is less susceptible to ice effects and is considered more accurate for the ice-cover season than the other two models, which are progressively more susceptible to ice effects.

*GLERL Contribution No. 260.

1. INTRODUCTION

The Detroit and St. Clair River dynamic flow models have been used for computing flows in the two rivers on various time scales for a number of years. These models, which disregard wind stress effects, are described by Quinn and Hagman (1977), but until recently, detailed comparisons of flows obtained for each river with different models had not been presented. A comparison for the Detroit River that analyzes flow differences due to hourly and daily computational time scales (intervals) and to wind stress effect modifications on both time scales is presented by Quinn (1980a). The wind stress effects are also described by Quinn (1980b). In the present study, there is a similar comparison for the St. Clair River flows, but in addition the St. Clair River models have been modified and recalibrated to provide better channel definition (improved resolution) and to include additional discharge measurements (1973 and 1977) that were not available during initial calibration. For comparison purposes, the improved models are designated as NEW, while previous models are designated as OLD. The flow comparison analysis is intended to serve as a guideline for the proper selection among the available models, with different configurations (wind, time scale) for specific applications.

2. PROCEDURE

The existing St. Clair River transient models (Quinn and Hagman, 1977) include complete one-dimensional equations of continuity and motion, but neglect the effects of wind stress and ice. The equations of continuity and motion are expressed in terms of flow and stage

$$\frac{\partial Z}{\partial t} + \frac{1}{T} \frac{\partial Q}{\partial X} = 0 \quad (1)$$

and

$$\frac{1}{A} \frac{\partial Q}{\partial t} - 2 \frac{Q}{A^2} \frac{\partial Z}{\partial t} + \left(g - \frac{Q^2 T}{A^3} \right) \frac{\partial Z}{\partial X} + \frac{g n^2 Q |Q|}{2.208 A^2 R^{4/3}} = 0, \quad (2)$$

where:

- Q = flow rate,
- Z = stage above a fixed datum,
- X = distance in the positive flow direction,
- t = time,
- A = channel cross-sectional area,
- T = water surface at top width of the channel,
- g = acceleration due to gravity,
- R = hydraulic radius, and
- n = Manning's roughness coefficient.

Modification for the wind stress effects was made using the common drag coefficient approach, following Quinn (1980b), by including the surface wind stress term in equation (2) for momentum, as follows:

$$\tau_w = \rho_a C_D U^2 \quad (3)$$

and

$$\frac{1}{A} \frac{\partial Q}{\partial t} - 2 \frac{Q T}{A^2} \frac{\partial Z}{\partial t} + \left(g - \frac{Q^2 T}{A^3} \right) \frac{\partial Z}{\partial x} + \frac{g n^2 Q}{2.208 A^2 R^{4/3}} \frac{Q}{R} - \frac{\rho_a}{\rho_w} \frac{U^2 \cos(\phi - \alpha)}{A} \cos(\phi - \alpha) C_D T = 0, \quad (4)$$

where:

- τ_w = surface wind stress term,
- ρ_a = air density ($1.25 \times 10^3 \text{ gm m}^{-3}$),
- C_D = drag coefficient (1.2×10^{-3}),
- U = wind velocity,
- ρ_w = water density ($1.0 \times 10^6 \text{ gm m}^{-3}$),
- ϕ = channel azimuth, and
- α = wind direction.

The value of the drag coefficient ($C_D = 1.2 \times 10^{-3}$) used in the wind stress calculations was determined during the International Field Year for the Great Lakes (IFYGL) investigations (Holland et al., 1981). The St. Clair River channel azimuths (ϕ) were determined for the mid-channel at various sections, generally following the United States-Canadian international boundary. The OLD St. Clair River flow models were composed of two equivalent channels, with three sections (two end sections and a mid-section used primarily for checking computed stages and flows). In the NEW models, with improved resolution, the number of sections was increased for better definition of the river channel. These new sections, with gage locations, hydraulic parameters, and channel azimuths, are listed in table 1. The wind data used in the analysis are the instantaneous hourly and resultant daily wind speeds and directions measured at the Sarnia Airport, Ont., for a 1-yr period (1977). Initially, 2 yr of data (1977-78) were tested, but the Fort Gratiot gage malfunctioned frequently during 1978 and so data for the second year had to be eliminated. The flow rates used in this study are those computed at the Mouth of Black River gage section, which for most models represents the mid-section.

TABLE I.--St. Clair River hydraulic parameters

Cage location	station (ft)	Width (ft)	Length (ft)	Azimuth (°)	Reference elevation IGLD (1955)"	Base area (ft ²)
Fort Gratiot (OLD)	207,970	1,800		30	576.7	57,500
	207,640	1,320	330	30	576.5	45,800
Duane Paper	207,090	1,000	550	30	576.4	40,800
	206,790	1,000	300	30	576.4	33,100
	206,350	1,000	440	30	576.3	35,000
	206,030	920	320	30	576.3	34,700
	205,320	880	710	30	576.1	28,800
	205,030	940	290	3	576.1	32,100
	204,600	1,000	430	3	576.1	33,400
	204,280	1,220	320	3	576.1	44,000
	203,970	1,360	313	3	576.1	49,700
	202,920	1,480	1,050	3	576.1	55,200
	202,570	1,520	350	161	576.1	65,600
	202,140	1,480	430	161	576.1	64,900
	200,840	1,400	1,300	161	576.0	48,200
	200,530	1,320	310	161	576.0	47,300
	199,520	1,360	1,010	143	575.9	53,100
199,240	1,360	280	143	575.9	50,200	
197,790	1,620	1,450	143	575.8	49,300	
Mouth of Black River	196,410	2,590	1,380	14	575.8	67,800
	195,410	2,630	1,000	14	575.8	76,000
	193,480	2,500	1,930	14	575.7	76,000
	190,400	1,840	3,080	31	575.7	50,700
Dry Dock	182,480	2,180	7,920	44	575.4	58,800
	170,920	1,890	11,560	14	575.1	57,100
Marysville	166,980	2,250	3,940	14	574.9	68,400
	166,480	2,400	500	18	574.9	68,300
	165,930	2,630	550	18	574.9	64,400
	163,380	3,490	2,550	1a	574.9	70,700
	162,810	3,290	570	18	574.9	71,600
	161,350	2,660	1,460	18	574.8	64,300
	155,470	2,640	5,880	177	574.7	62,600
	151,480	3,120	3,990	177	574.7	75,600
	148,430	2,420	3,050	10	574.5	65,900
	145,980	1,840	2,450	10	574.4	54,600
St. Clair (OLD)	144,970	1,960	1,010	10	574.4	61,500
	135,330	3,080	9,640	8	574.2	77,800
	134,290	2,760	1,040	8	574.1	65,600
St. Clair (NEW)	132,270	2,280	2,020	8	574.1	66,300

*IGLD--International Great Lakes Datum. Data in this table are listed in English units since all computations are done in English units and the final results listed in either English or SI system.

The various NEW and OLD St. Clair River models were run on both daily and hourly time scales for the whole year, and the resulting average daily flows were used in the comparison analysis. The NEW models were run both with and without the wind **stress** option. For this study, significant differences in flows are assumed when the average daily flow differences between **two** models or configurations are in excess of 2 percent, which represents the practical limit of accuracy for flow measurements. The comparison analysis was conducted for a total of five models, consisting of three available NEW models and two corresponding OLD models, all of which are listed below. Each model is designated by the upper, middle, and lower gages encompassing the upper and lower reaches of the models. These gages are as follows: Fort Gratiot (FG), Dunn Paper (DP), Mouth of Black River (MBR), Dry Dock (DD), and St. Clair (SC).

NEW MODELS: 1. FG-MBR-DD
 2. DP-MBR-DD
 3. MBR-DD-SC

OLD MODELS: 1. FG-MBR-DD
 3. MBR-DD-SC

3. RESULTS

3.1 Model Calibration

Calibration of the models consisted of computing the roughness coefficient, the unknown in the flow equation during periods of flow measurements, for each reach in the river representing upper and lower model reaches bounded by water level gages. The roughness coefficients for 14 **sets** of flow measurements conducted by the Corps of Engineers during 1959-77 were determined from Manning's formula

$$n = \frac{1.486 A R^{2/3}}{Q} \left(\frac{Z_u - Z_d}{L} + \frac{Q^2 \Delta A}{32.2 L A^3} \right)^{1/2}, \quad (5)$$

where:

- n** = Manning's roughness coefficient,
- A** = mean channel area,
- R** = hydraulic radius,
- Q** = flow rate,
- Z_u** = water surface at the upstream gage,
- Z_d** = water surface at the downstream gage,
- ΔA** = change in channel area from upstream to downstream gage, and
- L** = length of channel reach between upstream and downstream gages.

The relationships between computed roughness coefficients for channel reaches along the upper St. Clair River and the river stages at adjacent water level gages for the FG-MBR, DP-NBR, MBR-DD, and DD-SC reaches are shown in figures 1-4, respectively. From the relationships computed for the individual sets of discharge measurements, a common best-fit relationship was derived for each reach by regression analysis (least squares) or graphic plots (means), as shown in the figures. Some points were omitted in this derivation to eliminate possible gage errors or questionable measured flow values. The downstream reach (DD-SC) was affected by regimen changes between 1959 and 1963, when the shipping lane was dredged for navigational improvements. For this reach, a separate best-fit roughness coefficient was derived for each regime, representing pre-project conditions (through 1963) and current conditions (starting in 1964). The calibrated roughness coefficients for the four reaches are summarized in table 2.

The Fort Gratiot and St. Clair water level gages were moved in 1970, with apparent uncompensated hydraulic effects. Although an effort was made to measure any vertical change in the gage levels, there was a change in the apparent hydraulic regime because of the change in location and because of a difference in the river velocity at the new gage locations (Quinn, 1976). From a comparison study, Quinn found that water levels from the new Fort Gratiot gage should be reduced by 0.055 m (0.18 ft) and that water levels from the new St. Clair gage should be increased by 0.027 m (0.09 ft) to agree with the measurements taken prior to 1970. In the original transient model study (Quinn and Hagman, 1977), all the hydraulic computations of discharge equations and model calibrations were based on the original gage locations. In the present study, the hydraulic computations are based on a new St. Clair gage location, with the effect of this change on model derivation (Model 3) indicated in table 1. The original Fort Gratiot gage location was retained in the computations because the new gage displayed periods of erratic operations (which became quite frequent during 1978) and stopped operating completely during 1979.

3.2. Computer Programs

The revised St. Clair River models use water level and wind data from computer disk pack files. Two generalized versions for the daily and hourly models, respectively, were prepared and stored in the computer files, with options for various model versions (Model 1, 2, or 3), which can be operated either with or without wind input. The models, operated on hourly or daily computational time scales, also list average values for daily or monthly intervals, respectively. A seldom used monthly computational time scale for the monthly output option of the original models was eliminated. All basic data, data input, and hydraulic computations are in English units; the final results can be listed in either English or SI systems. The generalized daily St. Clair River dynamic flow model is listed in appendix A (figure A-44), and an example of the output is shown (table A-9).

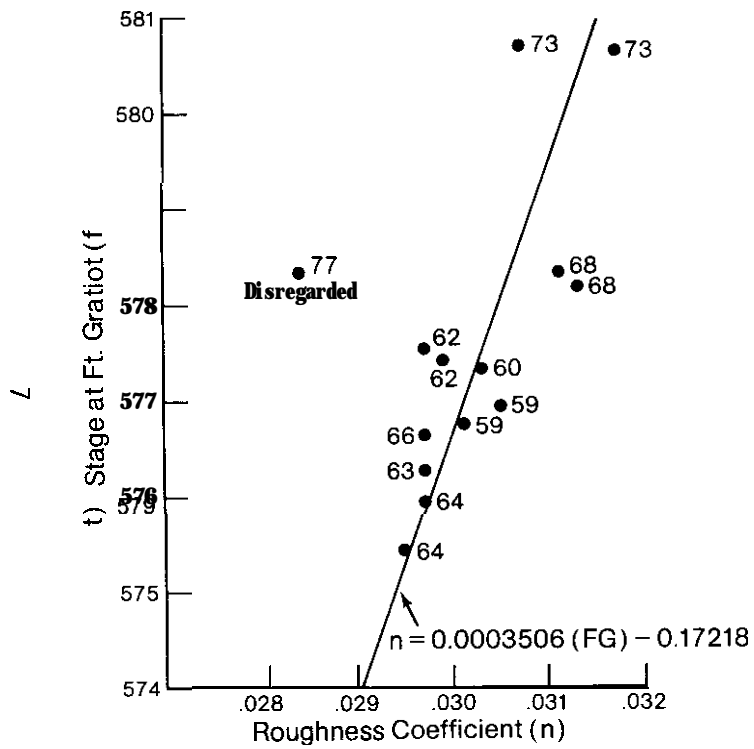


FIGURE 1.--Manning's roughness coefficient for the Fort Gratiot-Mouth Of Black River reach.

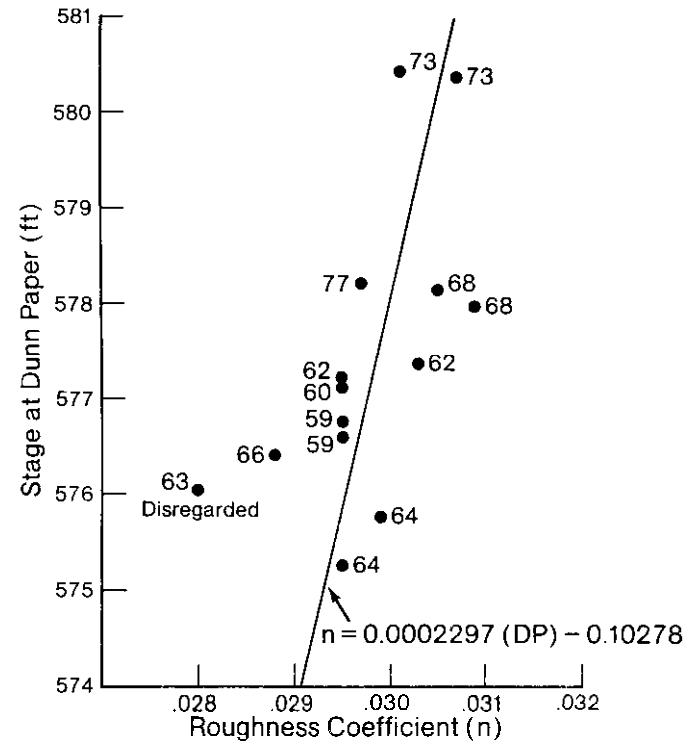


FIGURE 2.--Manning's roughness coefficient for the Dunn Paper-Mouth of Black River reach.

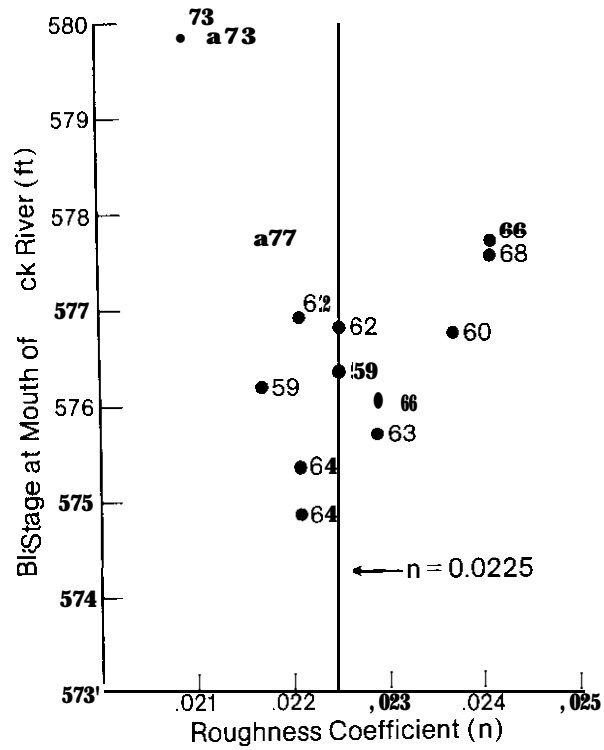


FIGURE 3.--Manning's roughness coefficient for the Mouth of Black River-Dry Dock reach.

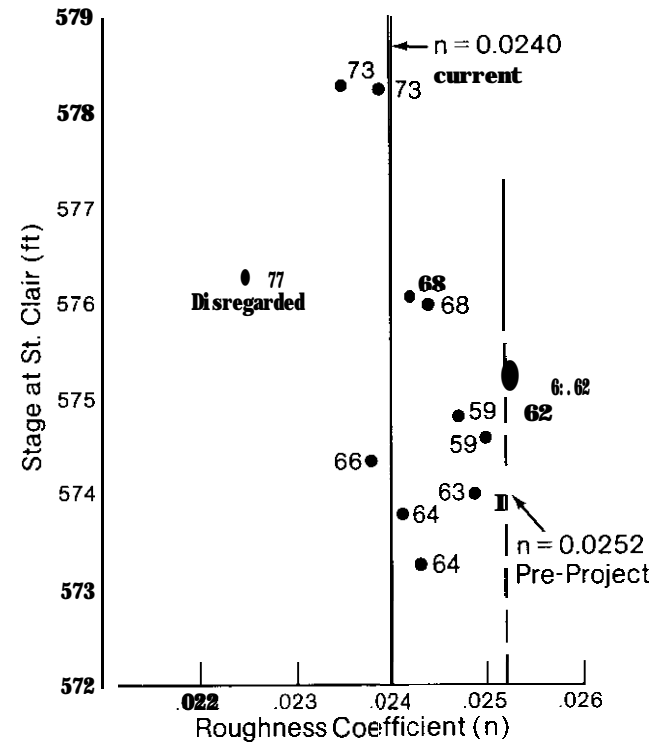


FIGURE 4.--Manning's roughness coefficient for the Dry Dock-St. Clair reach.

TABLE Z.--St. *Clair* River Manning's roughness coefficients

Reach	Roughness coefficient (n)
FG-MBR	n = 0.0003506 (FG) - 0.17218
UP-MBR	n = 0.0002297 (DP) - 0.10278
MBR-DD	n = 0.0225
DD-SC	a) Current regime: n = 0.0240 (starting in 1964)
	b) Pre-project regime: n = 0.0252 (through 1963)

3.3. Comparison of **NEW** and OLD Models

The effects of model improvements due to better resolution and additional flow measurements for model calibration are analyzed from comparison of daily flow differences, on both daily and hourly time scales, between the **NEW** and OLD models. Models 1 and 3, representing upper and lower models, respectively, are used in this comparison analysis, which excludes the wind option since OLD models do not have this capability. All comparisons of daily flow differences for each model configuration consist of histograms and cumulative frequency curves, which are designated (a) and (b), respectively, in the flow comparison figures. These flow comparison figures comprise 35 sets (a and b) of figures, which are placed on MICROFICHE attached to the report. Results for each major grouping of comparisons for the percentage of days with significant flow differences, defined as flow differences in excess of 2 percent of total flow, along with other designated percentages, are summarized in the accompanying tables. The 2 percent of flow value represents accuracy of flow measurements and indicates a practical zero difference for flow computations. During the period of study (1977), several water level gages had periods of missing data. All days with 6 or more hours of missing data for a particular model flow computation (upper and lower gages) were eliminated from the comparison of daily flow differences. The 6-hr restriction was selected from a comparison analysis, which showed that generally no additional accuracy in daily flows was obtained with more severe restrictions.

The effects of model improvements are shown in figures M-5 to M-8 and summarized in table 3. The NEW models produced somewhat higher flows, averaging about 3 percent for Model 1 and 4 percent for Model 3. These flow differences are quite consistent with relatively small scatter varying in range from 30 to 100 m³ s⁻¹ of flow differences, which represent from less than 1 percent to 2 percent of the average flow (part a of figures M-5 to M-8). With the offsets for flow increments, the histograms indicate reasonably close approximation of normal distribution for Model 1 but a positively skewed distribution for Model 3. This implies that flow differences from Model 3 are not random, which is contrary to what might be expected from normal natural phenomena. All flow differences between NEW and OLD models are significant, exceeding 2 percent of flow, but the frequency of occurrence is reduced drastically for flow differences in excess of slightly higher percentages of flow. The flow differences are eliminated at the 4-percent level in Model 1 and at the 5-percent level in Model 3 (part b of figures M-5 to M-8 and table 3). The use of daily or hourly time scales had little effect in Model 1, but a large effect in Model 3, where the flow differences are more persistent and the daily computational increments indicate considerable loss of accuracy (table 3).

TABLE 3.--Comparison of daily flows computed by NEW and OLD models: NEW - OLD

Model	Time scale	Percent of days with flow differences in excess of:			
		2%	3%	4%	5%
1	Daily	100	39	0	0
1	Hourly	100	41	0	0
3	Daily	100	100	100	0
3	Hourly	100	100	15	0

Additional examination of computed flows permits further evaluation of flow differences and indicates the reasons for their variation. Comparison of the average annual flows shows generally good agreement between NEW models, with nearly identical values from both time scales for each model. The agreement of average flows from the OLD models is less accurate. Both time scales produced lower (3 percent) but similar average flows in the OLD Model 1, while Model 3 daily computations produced about a 1-percent lower average value than hourly computations and the two values are 2-percent and 1-percent lower, respectively, than in Model 1. The combined effect of these differences is to produce flow differences between NEW and OLD models that attain 3 percent of average flow for Model 1, with both time scales, and average about 4 percent for Model 3, with nearly 1-percent negative difference between the hourly and daily time scales. Recalibration of NEW models produced results that are verified between both the models and the time scales, while OLD models produce significant flow differences between the models and a small time scale difference in Model 3. It appears that OLD Model 3 was undercalibrated, producing lower flows. The use of daily time scales in Model 3, spanning a reach of reduced river velocities, produced additional loss of accuracy in the OLD model, but eliminated it in the NEW model.

Past flow comparisons between different models (Derecki, 1978) show that the biggest flow differences normally occur during winter because of ice-cover and related backwater effects. Concentrated ice cover normally forms in the lower reaches of the St. Clair River, modifies the normal river profile with progressively decreasing effect upstream, and affects flow computations based on the normal river profile. The upper river reaches, having steeper slopes and being farther removed from ice concentrations, are less susceptible to ice-cover effects, and the upper models are considered to be more accurate during winter. This analogy also holds for the present comparison of different models, discussed in detail in the last section. The above analogy does not hold for the comparison of the same models with different configurations, because individual models are affected similarly by the ice effects regardless of configuration.

3.4. Wind Stress Effects

The effects of wind stress on daily flow computations with both daily and hourly time scales are analyzed from the comparison of individual NEW models (1-3), shown in figures M-V to M-14 and summarized in table 4. The impact of the wind stress term on daily flows is insignificant in Models 1 and 2, representing the upper reach of the river, but exerts a small influence in Model 3 for the lower reach. The resultant wind direction for the year (1977) was from the WSW (250°) and is aligned similarly with the general orientation of both reaches, which have an overall flow direction of 15°, varying from NNE to SSW. However, the lower reach is relatively straight, twice as long, and has reduced water velocities, allowing wind forces to exert more influence. The opposing directions of resultant wind and river flow (125°) tend to retard the flow, as indicated by a slight negative bias of the histograms. Since stronger winds are normally of short duration, models with hourly time scales also show slightly larger wind effects.

TABLE 4.--Comparison of wind *stress* effects on daily *flow* computations: *Wind - no wind*

Model	Time scale	Percent of days with flow differences in excess of 2%
NEW 1	Daily	0
1	Hourly	0
2	Daily	0
2	Hourly	0
3	Daily	1
3	Hourly	1

In Models 1 and 2 almost all flow differences are within $+ 50 \text{ m}^3 \text{ s}^{-1}$ and all within $+ 100 \text{ m}^3 \text{ s}^{-1}$, and all are below the 2-percent significant flow difference-(figures M-9 to M-12). In Model 3 the range of flow differences is twice as large, but nearly all flow differences are within 2 percent and all within 4 percent of the average **flow** (figures M-13 to M-14). The percentage of days with significant flow differences in Model 3 is 1 percent for both time scales (table 4). Generally, the wind stress term can be disregarded in computing daily flows with only slight overestimation of flow. However, wind effects may be significant during shorter periods and should be considered for hourly fluctuations of flow.

3.5. Time Scale Effects

The effects of daily and hourly computational time increments on daily flows were assessed by comparing flow differences between the two time scales obtained with various individual models. In the NEW models, both with and without wind configurations were used in this comparison, which is shown in figures M-15 to M-22 and summarized in table 5. The results are generally similar to those described for the wind stress effects, except that most histograms show a slight positive bias, which means that flows computed with the daily time scales are slightly higher. An exception to the above is the OLD Model 3 (figure M-22a), which shows a negative offset of about $40 \text{ m}^3 \text{ s}^{-1}$ in the distribution of flow differences. This amounts to nearly 1 percent of the average flow and indicates slightly lower flows for the daily time **scale**. It also **agrees** with results discussed previously in section 3.3.

TABLE 5.--Comparison Of *daily and hourly time scales on daily flow computations: Daily - hourly*

Model	Configuration	Percent of days with flow differences in excess of 2%
NEW 1	No wind	0
1	Wind	0
2	No wind	0
2	Wind	0
3	No wind	0
3	Wind	1
OLD 1	No wind	0
3	No wind	0

Most flow differences for various runs are confined within the range of $+ 50 \text{ m}^3 \text{ s}^{-1}$ and nearly all within $+ 100 \text{ m}^3 \text{ s}^{-1}$ or below the 2-percent significant flow difference. All models with the wind option are a little more sensitive to the time scale selection, showing a slightly increased range of flow differences, but only Model 3 indicates a significant increase in the number of flow differences in excess of 2 percent of average flow, with 1 percent (table 5). Thus, the St. Clair River flows for daily or longer periods can be computed by disregarding wind stress and using daily time scales, with only slight overestimation of the river discharge. Comparison results for this and the preceding section also show, that during more intensive short-period flow fluctuations, the effects of wind stress may be significant and should be considered.

3.6. Effect of Daily Winds on Hourly Models

The U.S. National Weather Service short-period wind data are normally stored for synoptic hours, at 3-hr intervals; hourly wind data are generally not available. In the present study, the Canadian hourly wind data were used, which permitted matching of the time scales between the models and wind data. However, one of the questions raised when modifying the models for the surface wind stress was the effect of different time scales on flow

computations. This effect was evaluated with resultant daily winds used in hourly models. Comparisons of daily flow differences computed with hourly models containing daily and hourly wind configurations are shown in figures M-23 to M-25 and summarized in table 6. The results show no significant differences or loss of accuracy in daily flow computations, but this comparison is mainly academic since neither wind nor time scales were very significant for daily flows.

3.7. Comparison of Different Models

Comparison of daily flows obtained with different models under various configurations is shown in figures M-26 to M-39 and summarized in table 7. The results show that daily flow differences between different models are much greater than any variations between the individual models, with only small influence exerted by various model configurations. The range of flow differences between different models is about 10 times greater than for the individual models. The extreme flow differences exceed $+ 1,000 \text{ m}^3 \text{ s}^{-1}$ or about 20 percent of the average flow between Model 1 and the other two models, but are reduced in half to about $+ 500 \text{ m}^3 \text{ s}^{-1}$ or 10 percent of the average flow between Models 2 and 3. All-histograms show reasonably close approximations of normal distribution, with a slight negative bias between Models 1 and 2 (figures M-26 to M-29), very little if any bias between Models 1 and 3 (figures M-30 to M-33a), and a slight positive bias with a reduced range of flow differences between Models 2 and 3 (figures M-34 to M-37a). The histograms for flow differences between the OLD Models 1 and 3 (part a of figures M-38 to M-39) also indicate some positive bias for the daily time scale, but the OLD Model 3 was shown previously to underestimate the flows, with larger underestimates at this time scale.

TABLE 6.--Comparison of *daily flows computed with hourly models* using daily and hourly winds: *Daily - hourly*

Model	Configuration	Percent of days with flows differences in excess of 2%
NEW 1	Hourly model, daily and hourly winds	0
2	Hourly model, daily and hourly winds	0
3	Hourly model, daily and hourly winds	0

TABLE 7.--Comparison of daily flows computed with different models and configurations

Model	Configuration	Percent of days with flow differences in excess of:					
		2%	5%	10%	15%		
NEW	1 - 2	Daily, no wind	54	23	5	3	
	1 - 2	Daily, wind	54	23	5	3	
	1 - 2	Hourly, no wind	54	22	6	3	
	1 - 2	Hourly, wind	53	22	6	3	
	1 - 3	Daily, no wind	48	26	9	3	
	1 - 3	Daily, wind	47	24	9	3	
	1 - 3	Hourly, no wind	50	24	9	3	
	1 - 3	Hourly, wind	47	24	9	3	
	2 - 3	Daily, no wind	35	5	1	0	
	2 - 3	Daily, wind	35	5	1	0	
	2 - 3	Hourly, no wind	36	5	1	0	
	2 - 3	Hourly, wind	38	5	1	0	
	OLD	1 - 3	Daily, no wind	57	23	7	3
		1 - 3	Hourly, no wind	49	22	7	2

Because of the large flow differences between different models, an unacceptably high percentage of days (46 percent) exceeded the 2-percent significant flow difference, as shown in the cumulative frequency curves and the summary table. Approximately one-quarter of the days could be attributed to winter season and related ice effects, while nearly one-half of the days for the combined comparison of all models exceeded the significant flow difference. The highest number of days with flow differences in excess of 2 percent of average flow was between Model 1 and 2, with 54 percent, followed closely by those between Model 1 and 3, with 48 percent, while the lowest

percentage was between Models 2 and 3, with 36 percent. These high frequencies of occurrence in the flow differences are reduced drastically for higher specified percentages of flow, but are not eliminated entirely even at the 15-percent level for comparisons involving Model 1 (3 percent), and the 10-percent level between Models 2 and 3 (1 percent). Without Model 1, the comparability between Models 2 and 3 is much better, attaining similar accuracy at about a 5-percent lower level of average flow.

The high frequency of significant flow differences is also drastically reduced for longer time periods, such as weekly or monthly flows, but the above comparisons indicate generally poor results from the models for computing daily flows, especially with Model 1. This contradicts previous evaluation results for the relative model accuracy, as well as past flow comparison studies (Derecki, 1978). Additional evaluation of monthly flows shows a greatly reduced frequency of larger differences than is indicated by the combined annual comparison of daily flows. Most monthly flows obtained with different models agree within 2 percent and the flow differences are frequently smaller than 1 percent. Larger flow differences are normally restricted to winter months. The comparison showed that all monthly flow differences during winter between the upper and lower models, sequentially, are negative and indicate ice effects. The larger flow differences are between Model 1 and the other models because the Fort Gratiot gage, located at the confluence of Lake Huron and the St. Clair River, is basically unaffected by ice conditions downstream, while all other river gages are. With the reduced river fall because of ice effects, Model 1 produces lower flows, while in other models the reduced river fall is counterbalanced by raised water levels at the gages involved. This shows that only Model 1 substantially eliminates the ice effects, and thus it is more accurate during winter.

Verification of ice effects during winter is provided by figures 40-42, which show daily water level differences or river falls for the upper and lower reaches of each model. The figures also show periods of missing gage data, with days of records either completely missing or eliminated by the 6-hr restriction. The figures clearly show that ice affected the normal river profile and consequently river flow throughout January, February, and December, although nearly all December data for Model 1 (Fort Gratiot) were missing. The missing data periods eliminated approximately 50 days from the daily flow comparisons between Model 1 and the other two models, and about a month between Models 2 and 3. Another feature shown by the figures is the periods of large fluctuations from the normal river profile during the open-water season, with contradicting trends (up or down) indicated by the two reaches comprising the model. These periods occurring during July, August, and November in the FG-MBR reach of Model 1 (figure 40) and a few days in July for the DP-MBR reach of Model 2 (figure 41) were identified as artificial fluctuations caused by the Fort Gratiot and Dunn Paper gage malfunctions. Another indication of the Fort Gratiot gage malfunctions is the daily water level differences between the Lake Huron gage at Lakeport and the Fort Gratiot gage (figure 43). A comparison of figures 40 and 43 shows that the fluctuations during July, August, and November have exactly opposite trends and must be caused artificially by the Fort Gratiot gage malfunctions. Figure 43 also shows that Fort Gratiot is not affected by ice

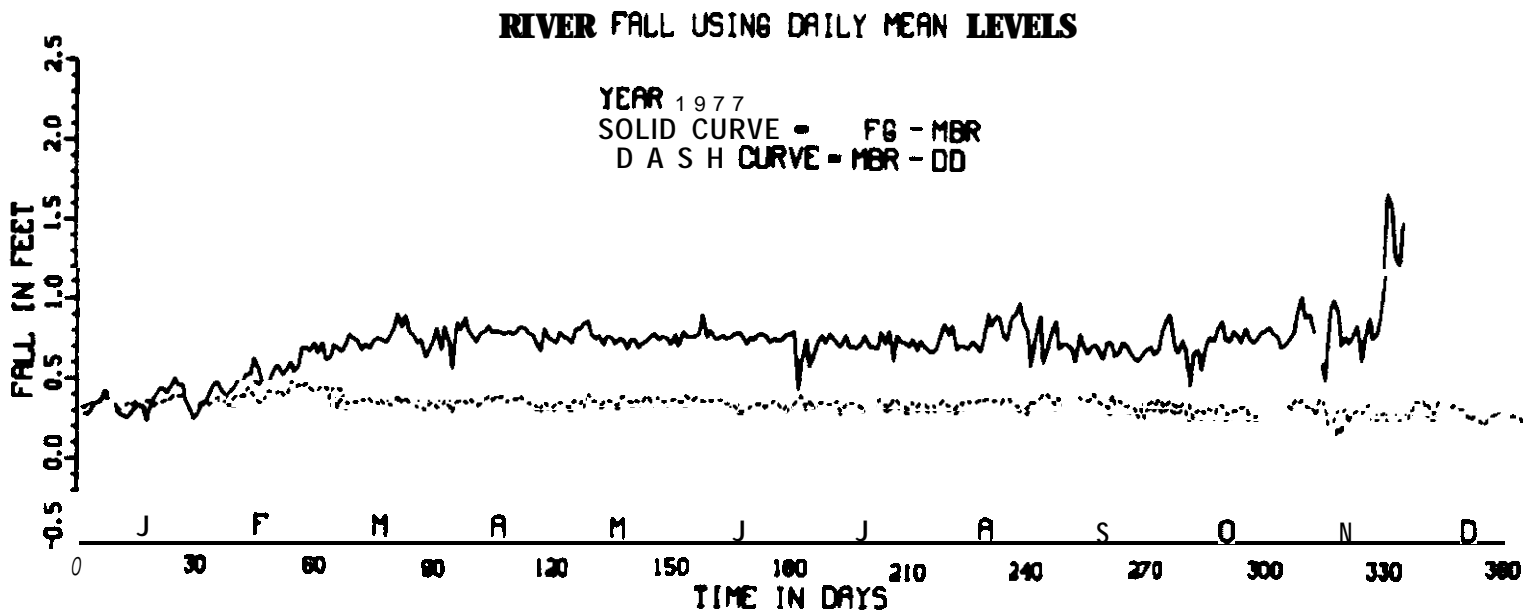


FIGURE 40.--Comparison of falls for upper and lower reaches of Model 1.

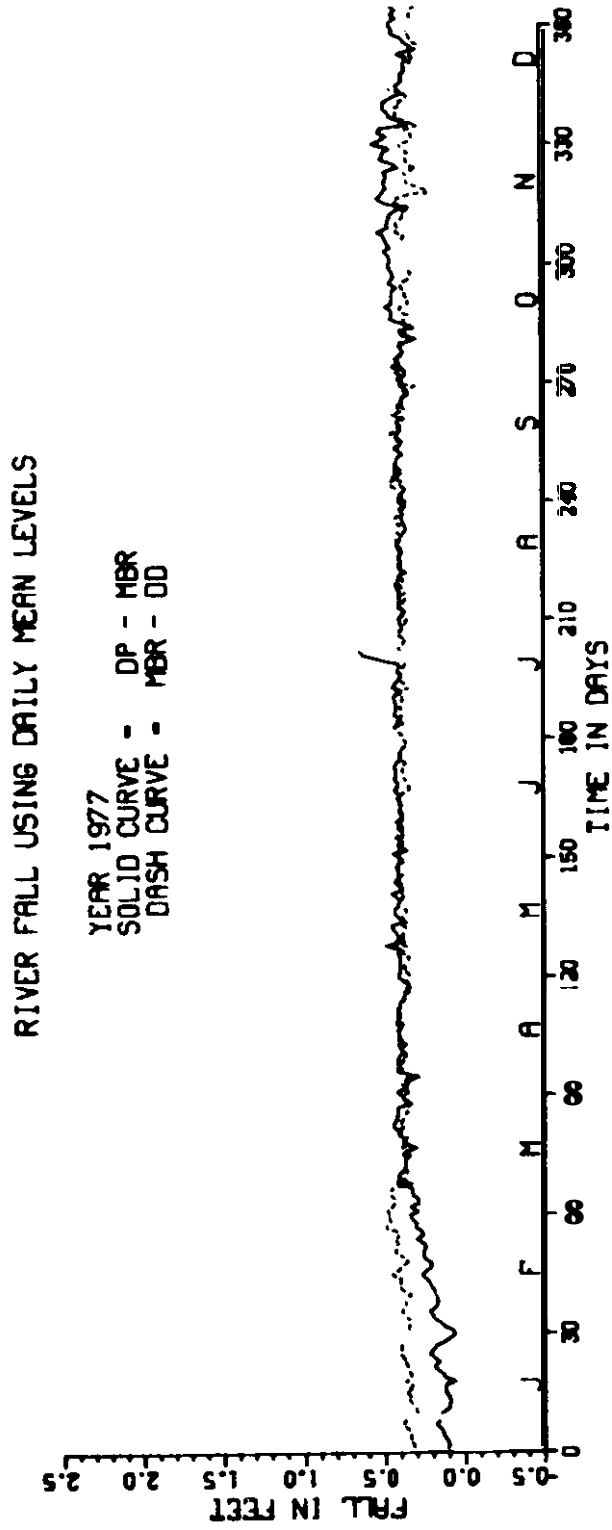


FIGURE 41 - Comparison of falls for upper and lower reaches of Model 2.

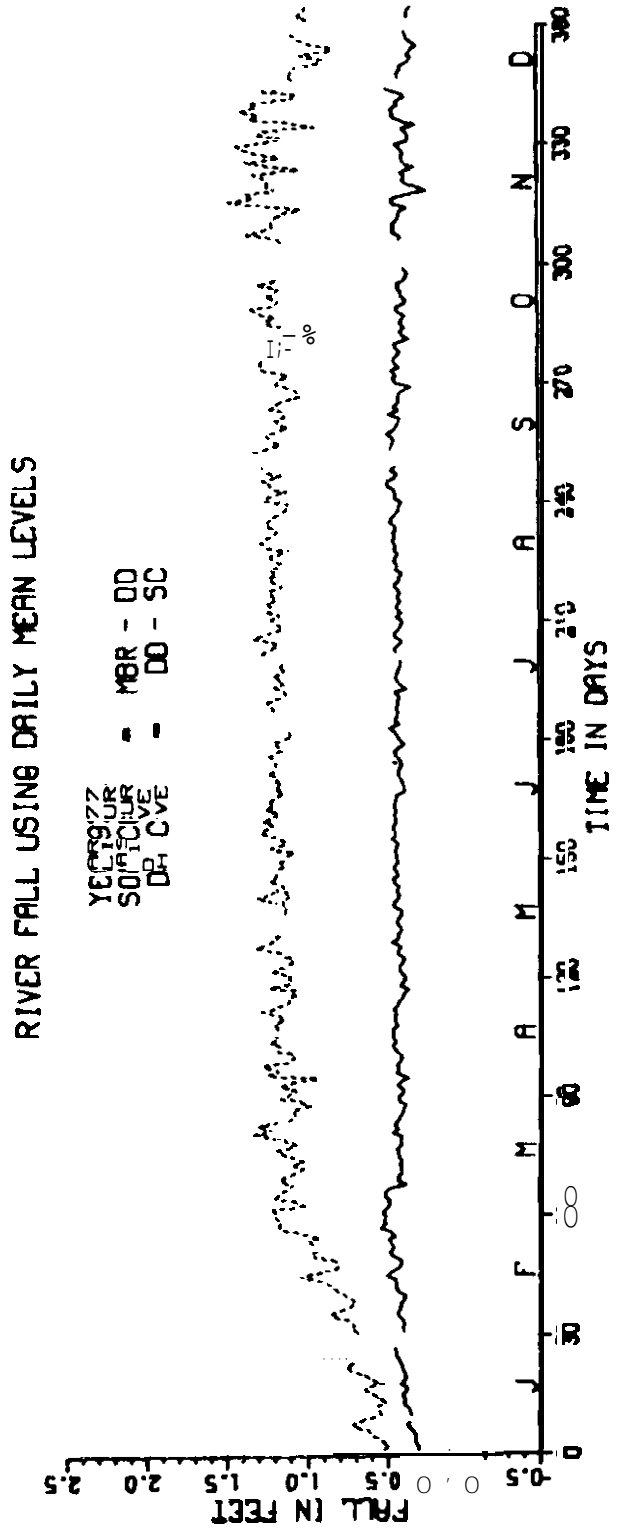


FIGURE 42 - Comparison of fall for upper and lower reaches of Model 3

RIVER FALL USING DAILY MEAN LEVELS

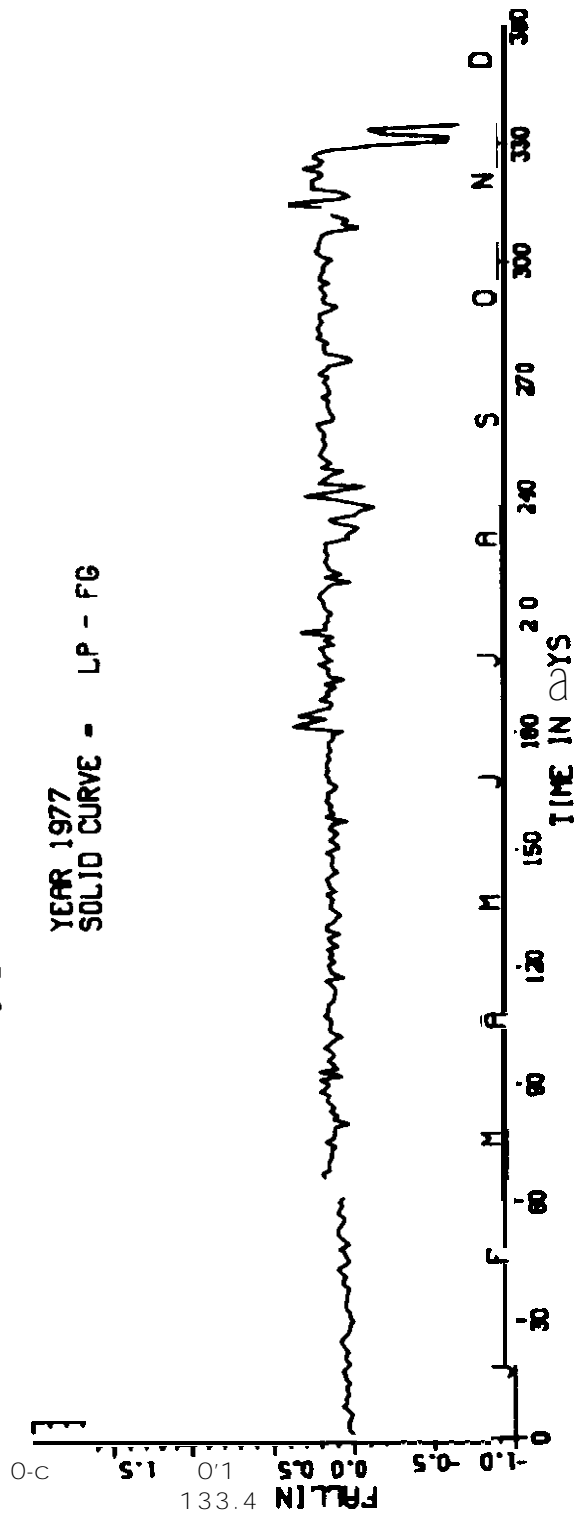


FIGURE 43 — Comparison of water level differences between Lakeport and Fort Gratiot gages.

conditions in the river. In contrast to these gage malfunctions, the natural variations in the river profile, such as those caused by ice effects during winter or winds, as in November for Models 2 and 3 (figures 41 and 42), show a similar trend in the fluctuations for both model reaches. The Fort Gratiot gage malfunctions during the 3 months eliminated an additional period of about a month from a valid comparison of daily flows involving Model 1. In the other two models, only a few additional days were eliminated.

The seasonal breakdown of daily flow differences between various models is indicated in table 8, which shows a comparison between annual, winter, and open-water seasons for the daily time scale and no wind configuration. This, the most basic configuration, was selected for the comparison since various configurations had little effect on daily flow computations. The table shows that there is practically no difference between the annual and seasonal values for Models 2 and 3, indicating that these models are not very sensitive to ice effects. In contrast, the flow differences between Model 1 and the other models show a very large ice effect during winter, verifying river conditions indicated in figures 40-42. The largest winter flow differences are between Models 1 and 3, indicating that Model 2 is a little more sensitive to ice effects than Model 3, but only Model 1 substantially eliminates ice effects. It is, therefore, essential that the Fort Gratiot gage be maintained in proper operating condition and Model 1 be available for winter flow computations. During the open-water season, flow differences between Model 1 and the other models are greatly reduced, and comparable between all models when corrected for gage malfunctions, primarily at Fort Gratiot. The accuracy of all models for daily flow computations is adequate at the 5-percent level of average flow, where only 3-4 percent of the days exceed that flow during the open-water season. The indicated large differences between the models are valid during the winter, since Models 2 and 3 are not very sensitive to ice effects, while Model 1 is, and thus is more accurate during winter. However, all models are calibrated for open-water conditions and require verification/recalibration for winter flows affected by ice, based on the actual river velocities.

4. CONCLUSIONS

This report describes current modifications for the St. Clair River dynamic flow models and presents flow comparisons to assist potential users in the selection of the proper model configuration for a particular application. The three available models can be operated on hourly or daily time scales, with and without surface wind stress effects. Generally, most users can be satisfied with daily models without the wind option, since both wind and time scales have little effect on daily or longer-period flows. For more intensive short-period flow fluctuations, hourly models with the wind option should be considered. During the open-water season, either of the three models can give satisfactory results, with the accuracy of various models within 5 percent for daily flows. During the winter, ice may affect the accuracy of flow computations and model differences may exceed 15 percent of daily flow; Model 1 (FG-MBR-DD) for the upper river reach is the

TABLE 8.--*Seasonal* comparison of *daily flows* computed by
 NEW models with configurations: Daily, no wind

Seasonal	Model	Percent of days with flow differences in excess of:			
		2%	5%	10%	15%
Annual	1 - 2	54	23	5	3
	1 - 3	48	26	9	3
	2 - 3	35	5	1	0
Winter	1 - 2	95	66	10	5
	1 - 3	100	82	30	7
	2 - 3	39	7	0	0
Open-water	1 - 2	45	14	4	2
	1 - 3	37	13	4	2
	2 - 3	34	4	1	0
Corrected*	1 - 2	37	4	0	0
open-water	1 - 3	29	4	0	0
	2 - 3	33	3	0	0

*Open-water correction based on elimination of isolated periods with water level gage malfunctions.

most suitable for eliminating ice effects, and it is therefore essential that the Fort Gratiot gage be maintained in proper operating condition. However, all models may contain some ice effect and should be recalibrated when winter river velocity measurements are available.

5. REFERENCES

- Derecki, J. A. (1978): Description of the method used by the Great Lakes Environmental Research Laboratory to determine flows in the St. Clair and Detroit Rivers for the River Flow Subcommittee, GLERL Open File Report, Great Lakes Environmental Research Laboratory, Ann Arbor, Mich. 48104. 20 pp.
- Holland, J. Z., Elder, F. C., Chen, W. Y., and Almazan, J. A. (1981): Atmospheric boundary layer. In *IFYGL--The International Field Year for the Great Lakes*. NOAA, Rockville, Maryland, (in press).
- Quinn, F. H. (1980a): Intercomparison analysis of Detroit River dynamic flow models, GLERL Open File Report, Great Lakes Environmental Research Laboratory, Ann Arbor, Mich. 48104. 16 pp.
- Quinn, F. H. (1980b): Note on wind stress effects on Detroit River discharges. *J. Great Lakes Res.* 6(2):172-175.
- Quinn, F. H., and Hagman, J. C. (1977): Detroit and St. Clair transient models, NOAA Tech. Memo. ERL GLERL-14, National Technical Information Service, Springfield, Va. 22151. 45 pp.
- Quinn, F. H. 1976: Effect of Fort Gratiot and St. Clair gage relocations on the apparent hydraulic regime of the St. Clair River, GLERL Open File Report, Great Lakes Environmental Research Laboratory, Ann Arbor, Mich. 48104. 7 pp.

Appendix A, GENERALIZED ST. CLAIR RIVER DAILY FLOW MODEL, INPUT, AND OUTPUT

INPUT: I. Time Scales--select generalized model with desired time scale.

A. (SCRFL0H)--Hourly

B. (SCRFL0)--Daily;

II. Options--specify numbered options in indicated sequence (A-C):

A. Model Selection:

(1)--Model 1, upper (FG-MBR-DD)

(2)--Model 2, middle (DP-XBR-DD)

(3)--Model 3, lower (MBR-DD-SC)

B. Wind Options:

(0)--Without wind

(1)--With wind

C. Output Units:

(0)--English

(1)--Metric (SI).

TABLE A-9.--St. Clair River daily model output for Model 1, with wind stress, metric, December, 1978

DAY	MON	MEAS. DD LEVEL	COMP. MBR LEVEL	COMP. DP LE "EL	MEAS. FG LEVEL	COMP. DD FLOW	COMP. MBR FLOW	COMP. FG FLOW	MEAS. MBR CHECK	(C-M) MBR DEV1	MEAS. DP CHECK	(C-M) DP DEV2	WIND VEL. KMH	WIND DIR. DEG.
1	12	175.97	176.10	176.25	176.32	5867.	5867.	5867.	176.10	.00	176.92E	-.67	10.3	240.
2	12	175.99	176.11	176.27	176.34	5962.	5963.	5965.	176.09	.03	176.92E	-.65	10.5	301.
3	12	175.89	175.99	176.12	176.17	5279.	527.	527.	176.05	-.06	176.92E	-.80	16.7	141.
4	12	175.86	175.94	176.04	176.09	4745.	4745.	4744.	175.96	-.02	176.92E	-.87	31.4	239.
	12	175.95	176.03	176.11	176.16	4495.	4498.	4501.	176.03	-.00	176.92E	-.81	24.3	216.
6	12	175.97	176.08	176.21	176.27	5397.	5397.	5398.	176.08*	.00	176.92E	-.71	10.0	265.
7	12	175.92	176.05	176.20	176.27	5806.	5804.	5803.	176.02.	.03	176.92E	-.72	9.5	119.
8	12	175.96	176.07	176.21	176.27	5576.	5578.	5579.	176.06	.01	176.92E	-.71	21.6	321.
9	12	175.93	176.11	176.26	176.33*	5858.	5859.	5860.	176.08	.03	176.92E	-.66	26.6	285.
10	12	175.98	176.11	176.26	176.33E	5916.	5916.	5915.	176.07	.03	176.92E	-.66	25.1	267.
11	12	175.9,	176.07	176.24	176.33'	6405.	6403.	6403.	176.01	.06	176.92E	-.67	15.1	197.
12	12	175.89	175.97	176.08	176.13*	4890.	4888.	4885.	175.97	.00	176.92E	-.84	20."	208.
13	12	175.97	176.08	176.20	176.26	5419.	5424.	5927.	176.04	.03	176.92E	-.72	31.4	257.
14	12	175.93	176.04	176.17	176.24*	5442.	5439.	5437.	176.02	.02	176.92E	-.75	28.2	230.
15	12	175.89	176.00	176.12	176.17	5222.	5221.	5220.	175.97	.03	176.92E	-.80	29.0	222.
16	12	175.91	176.03	176.17	176.24	5698.	5699.	5700.	175.49	.04	176.92E	-.75	14.8	201.
17	12	176.00	176.12	176.28	176.35	6001.	6004.	6006.	176.05	.08	176.92E	-.64	30.6	280.
18	12	175.95	176.00	176.23	176.31*	5979.	5977.	5975.	176.03	.05	176.21*	.02	9.2	336.
19	12	175.89	176.04	176.22	176.31E	6446.	6445.	6445.	175.40	.06	176.14	.08	7.9	108.
20	12	175.83	175.99	176.08	176.14	5446.	5443.	5440.	175.93	.01	176.06	.02	14.0	137.
21	12	175.90	176.00	176.12	176.18*	5270.	5274.	5276.	176.00	-.00	176.13	-.00	30.3	275.
22	12	175.86	175.96	176.07	176.12*	4993.	9990.	4988.	175.97	-.02	176.10	-.03	24.9	229.
23	12	175.92	176.03	176.16	176.22	5470.	5474.	5476.	176.03	.00	176.18	-.02	11.1	213.
24	12	175.83	175.94	176.07	176.14	5395.	5391.	5388.	175.94	-.00	176.08	-.00	12.6	149.
25	12	175.92	176.02	176.14	176.20	5290.	5295.	5298.	176.03	-.01	176.17	-.03	25.6	260.
26	12	175.92	176.04	176.18	176.25.	5647.	5646.	5646.	176.04	-.00	176.19	-.01	18.0	267.
27	12	175.92	176.05	176.19	176.26.	5781.	5781.	5781.	176.05	.00	176.19	.00	22.9	273.
28	12	175.91	176.09	176.20	176.27	5974.	5973.	5973.	176.03	.01	176.18	.02	5.0	234.
29	12	175.00	175.92	176.07	176.13	5589.	5584.	5581.	175.9,	.02	176.03	.03	21.6	124.
30	12	175.80	175.90	176.01	176.07	5048.	5048.	5049.	175.09	.00	176.03	-.02	14.2	159.
31	12	175.92	176.01	176.12	176.17	4964.	4968.	497.	176.03	-.02	176.18	-.06	5.7	45.
AVE		175.9,	176.03	176.16	176.23	5525.	5525.	5525.	176.01	.01	176.56	-.40		

25

NOTE: (*)--indicates partial records, with some missing data.
(E)--indicates estimates based on preceding periods for completely missing data.

```

PROGRAM SCRFLO (INPUT,OUTPUT,TAPE5=INPUT,TAPE6=OUTPUT,
1 TAPE22,TAPE23,TAPE24,TAPE11,TAPE14,TAPE15)
C UPPER ST. CLAI P RIVER UNSTEADY FLOY MODEL
C FRANK H. QUINN PROGRAMMER
COMMON IHOUR(24,31),MEAN(31),MEM,MAXV(31),MAXD(31)
COMMON MINH(31),MIND(31)
COMMON MAXM(4),MINM(4),IC,IGEAGE,MONAA,IYRR
DIMENSION AA(100),ABAS(100),DATU(100),AT(100),X(100),STA(80)
DIMENSION WS(50,80),Q(55,80),YVECT(160), XMTRX(160,160)
DIMENSION T(100),AN(100),A(100),U(100),R(100),QA(100)
DIMENSION SUM(12),AVE(12),ADJ(4),UW(80),ALPH(80)
DIMENSION IGAGE(4),ISET(4),AZ(100),AZM(100)
DIMENSION IPAR(80,31),UWD(730),ALPHD(730)
DIMENSION OLD(4)
DIMENSION BMTRX(160,5),XL(480)
DATA (STA(I),I=1,39)/132270.,134290.,135330.,144970.,145980.,
1148430.,151480.,155470.,161350.,162810.,163380.,165930.,166480.,
2166980.,170920.,182480.,190400.,193480.,195410.,196410.,
3197790.,199240.,199520.,200530.,200840.,202140.,202570.,202920.,
4203970.,24280.,204600.,205030.,205320.,206030.,206350.,206790.,
5207090.,207640.,207970./
DATA (ABAS(I),I=1,39)/66300.,65600.,77800.,61500.,54600.,65900.,
175600.,62600.,64300.,71600.,70700.,64400.,68300.,68400.,57100.,
258800.,50700.,76000.,76000.,67800.,49300.,
350200.,53100.,47300.,48200.,64900.,65600.,55200.,49700.,44000.,
433400.,32100.,28800.,34700.,35000.,33100.,40800.,45800.,57500./
DATA (DATU(I),I=1,39)/574.10,574.10,574.20,574.40,574.40,574.50,
1574.70,574.70,574.80,574.90,574.90,574.90,574.90,574.90,574.90,575.10,
2575.40,575.70,575.70,575.80,575.80,575.80,
3575.90,575.90,576.00,576.00,576.10,576.10,576.10,576.10,576.10,576.10,
4576.10,576.10,576.10,576.30,576.30,576.40,576.40,576.50,576.70/
DATA (AT(I),I=1,39)/2280.,2760.,3080.,1960.,1840.,2420.,3120.,
12640.,2660.,3290.,3490.,2630.,2400.,2250.,1890.,2180.,1840.,2500.,
22630.,2590.,1620.,1360.,1360.,1320.,1400.,1480.,1520.,1480.,1360.,
31220.,1000.,940.,880.,920.,1000.,1000.,1000.,1320.,1800./
DATA (AZ(I),I=1,39)/3*8.,3*10.,2*177.,5*18.,2*14.,44.,31.,3*14.,
13*143.,4*161.,5*3.,7*30./
DATA IGES/#EST #/
DATA IBLANK I# #/
DATA IAST /* #/
C
C READ BEGINNING YEAR AND MONTH; ENDING YEAR AND MONTH: MODEL,
C WIND AND METRIC OPTIONS# 715 FORMAT.
1 READ (5,1001) IYRA,MONA,IYRB,MONB,MODEL,IWIND,METRIC
IF (EOF(5)) 70,3
3 IF (IWIND.EQ.0) GO TO 100
C
C READ WINDS FROM DISC IN MPH AND DEGREES, 1977-1978.
IF (IYRA.EQ.1977.OR.IYRA.EQ.1978) GO TO 99
IF (IYRB.EQ.1977.OR.IYRB.EQ.1978) GO TO 99
GO TO 100
99 REWIND 14
REWIND 15
READ (14,1017) (UWD(J),J=1,730)
READ (15,1018) (ALPHD(J),J=1,730)
100 CONTINUE
C

```

FIGURE A-44.--Generalized St. Clair River daily flow model.

```

C      SELECT AND SET PARAMETERS FOR INDIVIDUAL REACHES
C      GO TO (101,102,103),MODEL
C
C      MODEL NO. 1, FG-DP-MBR-DO.
101  NRM=23
      NRAM=3
      NK 1=4
      NK2=22
      A1=0.
      B1=. 0225
      A2=. 0003506
      B2=-.17218
      IGAGE(1)=14087
      IGAGE(2)=14098
      IGAGE(3)=14090
      IGAGE(4)=14096
      OLD(1)=579.53
      OLD(2)=580.92
      OLD(3)=580.09
      OLD(4)=580.44
      I=16
      DO 111 J=1,24
      STA(J)=STA(I)
      ABAS(J)=ABAS(I)
      DATU(J)=DATU(I)
      AT(J)=AT(I)
      AZ(J)=AZ(I)
      I=I+1
111  CONTINUE
      GO TO 104
C
C      ROOEL NO. 2, DP-MBR-DD.
102  NRM=21
      NRAM=3
      NK 1=4
      NK2=0
      A1=0.
      B1=. 0225
      A2=. 0002297
      B2=-.10278
      IGAGE(1)=14087
      IGAGE(2)=14096
      IGAGE(3)=14090
      OLD(1)=579.53
      OLD(2)=580.44
      OLD(3)=580.09
      I=16
      DO 112 J=1,22
      STA(J)=STA(I)
      ABAS(J)=ABAS(I)
      DATU(J)=DATU(I)
      AT(J)=AT(I)
      AZ(J)=AZ(I)
      I=I+1
112  CONTINUE
      GO TO 104
C

```

FIGURE A-44. -- Continued.

```

C      MODEL NO. 3, MBR-DD-MV-SC.
103  NRM=18
      NRAM=15
      NK1=14
      NK2=16
      A1=0.
      B1=.0240
      A2=0.
      B2=.0225
      IGAGE(1)=14080
      IGAGE(2)=14090
      IGAGE(3)=14084
      IGAGE(4)=14087
      OLD(1)=578.50
      OLD(2)=580.09
      OLD(3)=579.01
      OLD(4)=579.53
104  CONTINUE
C
C      SET PARAYETERS COMMON TO ALL MODELS
      L=NRAN+1
      NMR=NRM+1
C      COMPUTE DISTANCES BETWEEN SECTIONS
      DO 4 I=1,NRM
        J=I+1
        4  X(I)=STA(J)-STA(I)
C
C      URITE BASIC DATA
      WRITE (6,3000)
      URITE (6,3010)
      URITE (6,3020)
      DO 41 I=1,NMR
        WRITE (6,3030) STA(I),ABAS(I),DATU(I),AT(I)
        IF (STA(I).EQ.132270.) URITE (6,3028)
        IF (STA(I).EQ.166980.) URITE (6,3029)
        IF (STA(I).EQ.182480.) WRITE (6,3031)
        IF (STA(I).EQ.195410.) URITE (6,3032)
        IF (STA(I).EQ.207090.) WRITE (6,3033)
        IF (STA(I).EQ.207970.) URITE (6,3034)
41  CONTINUE
      URITE (6,3035) A1,STA(1),B1
      URITE (6,3036) A2,STA(NMR),B2
      IFIRST = 0
      ISET(1) = 1
      ISET(2) = NWR
      ISET(3) = NMR+1
      ISET(4)=NMR+2
      ADJ(1)=0.
      ADJ(2)=0.
      ADJ(3)=0.
      ADJ(4)=0.
      NUR=NMR+1
      NURR=NMR+2
      ISTART = 13
      IEND = 43
      MX=5
      NX=6

```

FIGURE A-44. -- Continued.

```

NVAR=NRM*2
ANC=24.
DO 2 I=1,12
2 SUM(I)=0.
KKZ=11
AN(1)=.0235
TH=.75
TH1=.25
MM=0
M=13
KA=24
MON = MCNA
IYR = IYRA

C
C COME HERE EACH MONTH
2800 CONTINUE
C PRINT TITLES AND HEADINGS
WRITE(NX,3000)
10 WRITE(NX,1020)IYR
WRITE(NX,1021)ANC,NRM
IF(MODEL.EQ.2) GO TO 117
IF(MODEL.EQ.3) GO TO 417
YRITE(6,1025)
WRITE(NX,1125)
IF(METRIC.EQ.1) GO TO 217
WRITE(NX,1026)
GO TO 118
217 YRITE(6,1028)
GO TO 118
117 URITE(6,1225)
YRITE(6,1226)
IF(METRIC.EQ.1) GO TO 317
YRITE(6,1227)
GO TO 118
317 YRITE(6,1228)
GO TO 118
417 URITE(6,1025)
URITE(6,1326)
IF(METRIC.EQ.1) GO TO 517
YRITE(6,1026)
GO TO 118
517 URITE(6,1028)
118 CONTINUE

C
C READ WATER LEVELS FROM DISC.
IF(IYR.LT.1970.AND.MODEL.EQ.1) IGAGE(2)=14099
IF(IYR.LT.1971.AND.MODEL.EQ.3) IGAGE(1)=14081
IF(IYR.GE.1970.AND.MODEL.EQ.1) ADJ(2)=-.18
IF(IYR.LT.1971.AND.MODEL.EQ.3) ADJ(1)=-.09
IF(IYR.LT.1964.AND.MODEL.EQ.3) B1=.0252
JJJ=3
IF(NK2.GT.0) JJJ=4
DO 2005 JJ=1,JJJ
IW = 1
It = IGAGE(JJ)/10000
IGAG = IGAGE(JJ) - IC*10000
CALL GAGEIO(IW,IC,IGAG,MON,IYR,IB,IT,IDA,IDB,IDC,IER)

```

FIGURE A-44. --Continued.

```

      IF( IER) 60,5000,60
5000 CONTINUE
      KK = 1
      DO 2000 J=ISTART,IEND
      ICODE = IGAG
      DO 4000 I=1,24
C     FLAG MISSING DATA.
      IF( I HOUR(I, KK)) 4005,4005,4000
4000 IPAR(ISET(JJ),KK) = IBLANK
      GO TO 4010
4005 IPAR(ISET(JJ),KK) = IAST
4010 CONTINUE
      WS(J,ISET(JJ)) = 0.0
      IF( MEAN(KK) ) 6000,6000~6005
6000 WS(J,ISET(JJ)) = OLD(JJ)
      IPAR(ISET(JJ),KK) = IGES
      GO TO 6010
6005 CONTINUE
      WS(J,ISET(JJ))=(MEAN(KK) * I B )/100.0 +ADJ(JJ)
6010 CONTINUE
      OLD(JJ) = WS(J,ISET(JJ))
2000 KK = KK+1
2005 CONTINUE
C
C     READ WIND CARDS.
      CALL NODAYS( IYR,MON,1,NDM,NDY,JD)
      IF (IFIRST) 2500,2500,233
233 IF (IWIND.EQ.0) GO TO 23
      IF (IYR.EQ.1977.OR.IYR.EQ.1978) GO TO 165
      READ (5,1016) (UW(J),ALPH(J),J=2,13)
      READ (5,1016) (UW(J),ALPH(J),J=14,25)
      READ (5,1016) (UW(J),ALPH(J),J=26,32)
      DO 168 J=2,32
168 ALPH(J)=ALPH(J)*10.
      GO TO 23
165 IF (IYR.EQ.1978) NDY=NDY+365
      J2=NDY
      DO 169 J=2,32
      UW(J)=UWD(J2)
      ALPH(J)=ALPHD(J2)
      J2=J2+1
169 CONTINUE
      GO TO 23
2500 CONTINUE
      IF (IWIND.EQ.0) GO TO 107
      IF (IYR.EQ.1977.OR.IYR.EQ.1978) GO TO 170
      READ (5,1016) (UW(J),ALPH(J),J=13,24)
      READ (5,1016) (UW(J),ALPH(J),J=25,36)
      READ (5,1016) (UW(J),ALPH(J),J=37,43)
      DO 9 J=13,43
9 ALPH(J)=ALPH(J)*10.
      GO TO 107
170 IF (IYR.EQ.1978) NDY=NDY+365
      J2=NDY
      DO 172 J=13,43
      UW(J)=UWD(J2)
      ALPH(J)=ALPHD(J2)

```

FIGURE A-44. -- Continued.

```

      J2=J2+1
172  CONTINUE
107  DO 8 I=1,12
      UW(I)=UW(13)
      ALPH(I)=ALPH(13)
      WS(I,1)=WS(13,1)
      WS(I,NUR)=WS(13,NUR)
      WS(I,NURR)=WS(13,NURR)
      8 WS(I,NMR)=WS(13,NMR)
      DT=ANC*3600.
C**** INITIALIZE MATRIX *****
      DO 20 I = 1,NVAR
      DO 20 J = 1,NVAR
      20 XMTRX (I,J) = 0.
C**** DEFINE CONSTANT CHANNEL PARAHETERS * *****
      COMPUTE INITIAL CONDITIONS
      XSUM=0.
      DO 11 I=1,NRM
      11 XSUM=XSUM+X(I)
      SLOPE=(WS(1,NMR)-WS(1,1))/XSUM
      NRR=NRM-1
      DO 12 I=1,NRR
      J=I+1
      WS(1,J)=WS(1,I)+SLOPE*X(I)
      12 WS(2,J)=WS(1,J)
      DO 13 I=1,NMR
      QAA(I)= ABAS(I)+AT(I)+(WS(1,I)-DATU(I))
      13 CONTINUE
      DO 14 IJK=1,NMR
      JJ=IJK+1
      A(IJK)=(AA(IJK)+AA(JJ))/2.
      T(IJK)=(AT(IJK)+AT(JJ))/2.
      AZH(IJK)=(AZ(IJK)+AZ(JJ))/2.
      R(IJK)=A(IJK)/T(IJK)
      14 CONTINUE
      DO 17 I=1,NRM
      IF(I-NRAN) 15,15,16
      15 AN(I)=A1*WS(M,1)+B1
      60 TO 17
      16 AN(I)= A2*WS(M,NMR)+B2
      17 CONTINUE
      Q(1,1) =1.486*A(1)*R(1)**(2./3.)*(WS(1,2)-WS(1,1))**.5/AN(1)
      1/X(1)**.5
      DO 18 I=2,NMR
      Q(2,I)=Q(1,1)
      18 Q(1,I)=Q(1,1)
      KB=48
      M=1
      23 CONTINUE
      N = M+1
      LL=1
      21 CONTINUE
      DO 19 I=1,NRM
      ID=I
      IU=I+1
      QA(I)=TH/2.*(Q(N,ID)+Q(N,IU))+TH1/2.*(Q(M,ID)+Q(M,IU))
      19 U(I)=ABS(QA(I))

```

FIGURE A-44. -- Continued.

```

OO 7 I=1,NRM
IF(I-NRAN) 5, 5, 6
5 AN(I)=A1*WS(M,1)+B1
GOTO 7
6 AN(I)= A2*WS(M,NMR)+B2
7 CONTINUE
C**** COMPUTE AREAS AND HYDRAULIC RADIUS * *****
DO 24 I=1,NMR
QAA(I)= ABAS(I)+AT(I)*(TH*WS(N,I)+TH1*WS(M,I) -DATU(I))
24 CONTINUE
DO 22 IJK=1,NMR
JJ=IJK+1
A(IJK)=(AA(IJK)+AA(JJ))/2.
T(IJK)=(AT(IJK)+AT(JJ))/2.
AZM(IJK)=(AZ(IJK)+AZ(JJ))/2.
R(IJK)=A(IJK)/T(IJK)
22 CONTINUE
NR=NRM+2
C CONTINUITY EQUATIONS
NRD=NR-1
DO 26 I=1,NRD,2
II=I/2+1
ID=II
IU=ID+1
DYVECT(I)=-((WS(N,ID)+WS(N,IU)-WS(M,ID)-WS(M,IU))/(2.*DT)+(TH*(Q(N,
1ID) -Q(N,IU))+TH1*(Q(M,ID)-Q(M,IU)))/(T(II)*X(II)))
XMTRX(I,I)=TH/(T(II)*X(II))
XMTRX(I,I+2)=-XMTRX(I,I)
IF(I .GT. 1) GO TO 25
XMTRX(1,2)=1./(2.*DT)
GO TO 26
25 XMTRX(I,I-1)=1./(2.*DT)
XMTRX(I,I+1)=1./(2.*DT)
IF(I .EQ. NRD) XMTRX(I,I+1)=XMTRX(I,I+2)
IF (I.EQ.NRD) XMTRX(I,I+2)=0.
26 CONTINUE
C MOMENTUM EQUATIONS
OO 27 I=2,NR,2
II=I/2
ID=II
IU=ID+1
OZ41=-QA(II)*T(II)*(WS(N,IU)+WS(N,ID)-WS(M,IU)-WS(M,ID))/(2.*DT*A(I
1I)**2.)+2.
Z61=(Q(N,ID)+Q(N,IU)-Q(M,ID)-Q(M,IU))/(2.*DT*A(II))
Z11=32.2*AN(II)**2.*QA(II)*U(II)/(2.2082*A(II)**2.*R(II)**(4./3.))
Z21=32.2*(TH*(WS(N,ID)-WS(N,IU))+TH1*(WS(M,ID)-WS(M,IU)))/X(II)
Z31=-QA(II)**2.*(AA(ID)-AA(IU))/(A(II)**3.*X(II))
UW1=UW(M)*COS(.017453*(AZM(M)-ALPH(M)))*ABS(UW(M)*COS(.017453*
1(AZM(M)-ALPH(M))))*2.152
UW2=UW(N)*COS(.017453*(AZM(N)-ALPH(N)))*ABS(UW(N)*COS(.017453*
1(AZM(N)-ALPH(N))))*2.152
UR=(UW1+UW2)/2.
YVECT(I)=-Z11+Z21+Z31+Z41+Z61+1.500E-6*UR*T(ID)/A(ID)
OXMTRX(I,I)=-((32.2-QA(II)**2.*T(II)/(A(II)**3.))/X(II)+TH-QA(II)
1*T(II)/(DT*A(II)**2.))
IF(I .LT. 4) GO TO 29
OXMTRX(I,I-2)= (32.2-QA(II)**2.*T(II)/(A(II)**3.))/X(II)+TH-QA(II)

```

FIGURE A-44. -- Continued.

```

1*T(II)/(DT*A(II)**2.)
29 ZZZ1=ABS(QA(II))
OP1=32.2*AN(II)**2.*ZZZ1*TH/(2.2082*A(II)**2.*R(II)**(4./3.))-QA(II
1) /A(II)**3.*( AA(ID)-AA(IU) )
2*TH/X(II)-TH*T(II)*(WS(N, ID)+WS(N, IU)-WS(M, ID)-WS(M, IU))/(2.*DT*
3A(II)**2.)
XMTRX(I, I-1)=1./(2.*A(II)*DT)+P1
XMTRX(I, I+1)=XMTRX(I, I-1)
IF(I .EQ. NR) XMTRX(I, I)=XMTRX(I, I+1)
IF (I.EQ.NR) XMTRX(I, I+1)=0.
27 CONTINUE
C*** PRINT OUT MATRIX *****
DO 201 NN=1, NVAR
DO 201 J=1, 5
I=J+NN-3
IF(I)203,203,204
203 BMTRX(NN, J)=0.
GO TO 201
204 BMTRX(NN, J)=XMTRX(NN, I)
201 CONTINUE
CALL LEQT1B(BMTRX, NVAR, 2, 2, 160, YVECT, 1, 160, 0, XL, IER)
NNR=NR+1
C
DO 260 I=1, NNR, 2
II=I/2+1
IF(II-NMR)259,258,259
258 Q(N, NMR)=Q(N, NMR)+YVECT(NR)
C
CD TO 260
259 Q(N, II)=Q(N, II)+YVECT(I)
C
260 CONTINUE
NNR=NR-2
DO 265 I=2, NNR, 2
II=I/2+1
WS(N, II)=WS(N, II)+YVECT(I)
265 CONTINUE
LL=LL+1
LV=5
OO 266 I=2, NNR, 2
YVE=ABS(YVECT(I))
IF(YVE .GT. .002) LV=1
266 CONTINUE
IF(LV-5)21,50,50
50 CONTINUE
JB=N+1
IF (WS(N, NUR).LT.50.) WS(N, NUR)=WS(N, NK1)-.0000001
IF (NK2.LT.1) GO TO 151
IF (WS(N, NURR).LT.50.) WS(N, NURR)=WS(N, NK2)-.0000001
151 DEV1=WS(N, NK1)-WS(N, NUR)
IF(NK2.GT.0) DEV2=WS(N, NK2)-WS(N, NURR)
MM=MM+1
NM=MM-KKZ
IF(NM)57,57,53
C
C CONVERT ENGLISH TO METRIC.
53 IF (METRIC.EQ.0) GO TO 54

```

FIGURE A-44. -- Continued.

```

CONV1=WS(N,1)/3.28083
CONV2=WS(N,NK1)/3.28083
IF(NK2.GT.0) CONV3=WS(N,NK2)/3.28083
CONV4=WS(N,NMR)/3.28083
CONV5=Q(N,1)*.02832
CONV6=Q(N,L)*.02832
CONV7=Q(N,NMR)*.02832
CONV8=WS(N,NUR)/3.28083
CONV9=CONV2-CONV8
CONV10=WS(N,NURR)/3.28083
CONV11=CONV3-CONV10
CONV12=UW(N)*1.60935

C
C
C
PRINT OUTPUT.

IF TMODEL.EQ.2) GO TO 153
WRITE (6,1045) NM,MON,CONV1,IPAR(1,NM),CONV2,CONV3,CONV4,
1IPAR(ISET(2),NM),CONV5,CONV6,CONV7,CONV8,IPAR(ISET(3),NM),CONV9,
2CONV10,IPAR(ISET(4),NM),CONV11,CONV12,ALPH(N)
GO TO 55
153 WRITE (6,1046) NM,MON,CONV1,IPAR(1,NM),CONV2,CONV4,
1IPAR(ISET(2),NM),CONV5,CONV6,CONV7,CONV8,IPAR(ISET(3),NM),CONV9,
2CONV12,ALPH(N)
GO TO 55
54 IF (MODEL.EQ.2) GO TO 154
WRITE (6,1045) NM,MON,WS(N,1),IPAR(1,NM),WS(N,NK1),WS(N,NK2),
1WS(N,NMR),IPAR(ISET(2),NM),Q(N,1),Q(N,L),Q(N,NMR),WS(N,NUR),
2IPAR(ISET(3),NM),DEV1,WS(N,NURR),IPAR(ISET(4),NM),DEV2,UW(N),
3ALPH(N)
GO TO 55
154 WRITE (6,1046) NM,MON,WS(N,1),IPAR(1,NM),WS(N,NK1),WS(N,NMR),
1IPAR(ISET(2),NM),Q(N,1),Q(N,L),Q(N,NMR),WS(N,NUR),IPAR(ISET(3),NM)
2,DEV1,UW(N),ALPH(N)

C
C
COMPUTE MEAN VALUES.
55 SUM(1)=SUM(1)+WS(N,1)
SUM(2)=SUM(2)+WS(N,NK1)
IF(NK2.GT.D) SUM(3)=SUM(3)+WS(N,NK2)
SUM(4)=SUM(4)+WS(N,NMR)
SUM(5)=SUM(5)+Q(N,1)
SUM(6)=SUM(6)+Q(N,L)
SUM(7)=SUM(7)+Q(N,NMR)
SUM(8)=SUM(8)+WS(N,NUR)
SUM(9)=SUM(9)+DEV1
SUM(10)=SUM(10)+WS(N,NURR)
SUM(11)=SUM(11)+DEV2
57 DO 58 I=1,NMR
58 Q(JB,I)=2.*Q(N,I)-Q(M,I)
DO 51 I=2,NRM
51 WS(JB,I)=2.*WS(N,I)-WS(M,I)
M=M+1
IF( M-KB) 2333,2333,59
2333 CONTINUE

C
C
DAILY RETURN LOOP.
IF( NM-NOM) 23,59,59
59 CONTINUE

```

FIGURE A-44. -- Continued.

```

52 DO 65 I=1,11
65 AVE(I)=SUM(I)/NM
   IF (METRIC.EQ.0) GO TO 66
C
C   CONVERT WEANS TO METRIC
AVE(1)=AVE(1)/3.28083
AVE(2)=AVE(2)/3.28083
AVE(3)=AVE(3)/3.28083
AVE(4)=AVE(4)/3.28083
AVE(5)=AVE(5)*.02832
AVE(6)=AVE(6)*.02832
AVE(7)=AVE(7)*.02832
AVE(8)=AVE(8)/3.28083
AVE(9)=AVE(2)-AVE(8)
AVE(10)=AVE(10)/3.28083
AVE(11)=AVE(3)-AVE(10)
C
C   PRINT MEAN VALUES.
66 IF tMODEL.EQ.2) GO TO 67
   WRITE (6,1060) (AVE(I),I=1,11)
   GO TO 68
67 WRITE (6,1061) AVE(1),AVE(2),AVE(4),AVE(5),AVE(6),AVE(7),AVE(8),
1AVE(9)
C
68 IF (IYR-IYRB)5150,5100,60
5100 IF (MON-MONB)5150,60,60
5150 CONTINUE
   IF (MON-12)3200,3100,3100
3100 IYR=IYR+1
3200 CONTINUE
   DO 69 I=1,12
69 SUM(I)=0.
   DO 63 I=1,NMR
   WS(1,I)=WS(M,I)
   Q(1,I)=Q(M,I)
63 Q(2,I)=Q(JB,I)
   DO 64 I=2,NRM
64 WS(2,I)=WS(JB,I)
C   UPDATE MONTH AND YEAR
MON = MON+1
   IF (NON-131 21001 2150,2150
2150 MON=1
C   CHECK TO SEE IF ANY MORE DATA SHOULD BE PROCESSED
2100 IF ( IYR-IYRB)2300,2200,60
2200 IF ( MON-MONB) 2300.2300460
2390 CONTINUE
   MM=0
   KKZ=0
   M = 1
   KB=36
   ISTART = 2
   IEND = 32
   IFIRST = 1
C
C   MONTHLY RETURN LOOP.
GO TO 2800
C

```

FIGURE A-44. -- Continued.

```

C      NEU PARAMETERS OR END PROGRAM LOOP.
65    GO TO 1
C      PROGRAM ENDS FPOM EOF IN LABEL NO. 1.
70    STOP
C**** FORMAT STATEMENTS *****0501
1001  FORMAT (7I5)
1016  FORMAT (20X,12(F3.1,F2.0))
1017  FORMAT (F4.1)
1018  FORMAT (F4.0)
1020  FORMAT(////45X, #ST. CLAIR RIVER TRANSIENT MODEL#, //, 57X, I5, //)
1021  FORMAT (36X, F5.1, 1X, #HOUR TIME INCREMENTS#, 11X, I3, 1X, #REACHES#, //)
1025  FORMAT (19X, #MEAS.#, 4X, #COMP.#, 3X, #COMP.#, 3X, #MEAS.#, 5X, #COMP.#,
14X, #COMP.#, 4X, #COMP.#, 3X, #MEAS.#, 4X, # (C-M)#, 3X, #MEAS.#, 2X, # (C-M)#,
23X, #WIND#, 3X, #WIND#)
1125  FORMAT (21X, #DD#, 6X, #MBR#, 6X, #DP#, 6X, #FG#, 7X, #DD#, 7X, #MBR#, 6X, #FG#
1, 6X, #MBR#, 6X, #MBR#, 6X, #DP#, 5X, #DP#, 4X, #VEL.#, 3X, #DIR.#)
1526  FORMAT (8X, #DAY#, 2X, #MON#, 3X, #LEVEL#, 4X, #LEVEL#, 3X, #LEVEL#, 3X,
1#LEVEL#, 5X, #FLOW#, 5X, #FLOW#, 5X, #FLOW#, 4X, #CHECK#, 5X, #DEV1#, 3X,
2#CHECK#, 3X, #DEV2#, 4X, #MPH#, 3X, #DEG.#, /)
1028  FORMAT (8X, #DAY#, 2X, #MON#, 3X, #LEVEL#, 4X, #LEVEL#, 3X, #LEVEL#, 3X,
1#LEVEL#, 5X, #FLOW#, 5X, #FLOW#, 5X, #FLOW#, 4X, #CHECK#, 5X, #DEV1#, 3X,
2#CHECK#, 3X, #DEV2#, 4X, #KMH#, 3X, #DEG.#, /)
1045  FORMAT (6X, 2(2X, I3), 2X, F6.2, A1, 3(2X, F6.2), A1, 3(2X, F7.0), 2X, F6.2,
1A1, 2(2X, F6.2), A1, F6.2, 3X, F4.1, 3X, F4.0)
1046  FORMAT (16X, 2(2X, I3), 2X, F6.2, A1, 2X, F6.2, 2X, F6.2, A1, 3(2X, F7.0), 2X,
1F6.2, A1, 2X, F6.2, 3X, F4.1, 3X, F4.0)
1060  FORMAT (/, 8X, #AVE#, 7X, F6.2, 3X, F6.2, 2(2X, F6.2), 3X, F7.0, 2(2X, F7.0),
12X, F6.2, 1X, 2(2X, F6.2), 1X, F6.2)
1061  FORMAT (/, 18X, #AVE#, 7X, F6.2, 3X, F6.2, 2X, F6.2, 1X, 3(2X, F7.0), 2X, F6.2,
13X, F6.2)
1225  FORMAT (29X, #MEAS.#, 4X, #COMP.#, 3X, #MEAS.#, 5X, #COMP.#, 4X, #COMP.#,
14X, #COMP.#, 3X, #MEAS.#, 5X, # (C-M)#, 3X, #WIND#, 3X, #WIND#)
1226  FORMAT (30X, #DD#, 7X, #MBR#, 5X, #DP#, 8X, #DD#, 7X, #MBR#, 6X, #DP#, 6X,
1#MBR#, 7X, #MBR#, 4X, #VEL.#, 3X, #DIR.#)
1227  FORMAT (18X, #DAY#, 2X, #MON#, 3X, #LEVEL#, 4X, #LEVEL#, 3X, #LEVEL#, 5X,
1#FLOW#, 5X, #FLOW#, 5X, #FLOW#, 4X, #LEVEL#, 5X, #DEV1#, 4X, #MPH#, 3X, #DEG.#
2, /)
1228  FORMAT (18X, #DAY#, 2X, #MON#, 3X, #LEVEL#, 4X, #LEVEL#, 3X, #LEVEL#, 5X,
1#FLOW#, 5X, #FLOW#, 5X, #FLOW#, 4X, #LEVEL#, 5X, #DEV1#, 4X, #KMH#, 3X, #DEG.#
2, /)
1326  FORMAT (21X, #SC#, 7X, #MV#, 6X, #DD#, 5X, #MBR#, 7X, #SC#, 8X, #DD#, 6X, #MBR#
1, 6X, #MV#, 7X, #MV#, 6X, #DD#, 5X, #DD#, 4X, #VEL.#, 3X, #DIR.#)
3'00  FORMAT(1H1)
3010  FORMAT (///, 26X, #ST. CLAIR RIVER TRANSIENT MODEL#, /, 36X, #BASIC DAT
1A#)
3020  FORMAT (/, 23X, #STATION#, 5X, #ABASE#, 5X, #DATUM#, 5X, #WIDTH#, /)
3028  FORMAT (#+#, 62X, #ST. CLAIR#)
3029  FORMAT (#+#, 62X, #MARYSVILLE#)
3030  FORMAT (20X, F10.0, F19.0, F10.2, F10.0)
3031  FORMAT (#+#, 62X, #DRY DOCK#)
3032  FORMAT (#+#, 62X, #MOUTH BLACK RIVER#)
3033  FORMAT (#+#, 62X, #DUNN PAPER#)
3034  FORMAT (#+#, 62X, #FORT GRATIOT#)
3035  FORMAT (///, 12X, #DOWNSTREAM ROUGHNESS' N =#, F9.7, # . STA#, F7.0, # +
1#, F8.5)
3036  FORMAT (14X, #UPSTREAM ROUGHNESS' N =#, F9.7, # . STA#, F7.0, # +#, F8.
15)
      END

```

FIGURE A-44.--Continued.